The Astrophysical Journal Supplement Series, 189:240–252, 2010 July doi:10.1088/0067-0049/189/1/240

THE JINA REACLIB DATABASE: ITS RECENT UPDATES AND IMPACT ON TYPE-I X-RAY BURSTS

Richard H. Cyburt[1,2,9], A. Matthew Amthor[1,2,3], Ryan Ferguson[1,2,3], Zach Meisel[1,2,3], Karl Smith[1,2,3], Scott Warren[1,2,4], Alexander Heger[1,5], R. D. Hoffman[6], Thomas Rauscher[7], Alexander Sakharuk[1,2], Hendrik Schatz[1,2,3], F. K. Thielemann[7], and Michael Wiescher[1,8]
[1] Joint Institute for Nuclear Astrophysics (JINA), http://www.jinaweb.org
[2] National Superconducting Cyclotron Laboratory, Michigan State University, East Lansing, MI 48824, USA
[3] Department of Physics and Astronomy, Michigan State University, East Lansing, MI 48824, USA
[4] Department of Electrical and Computer Engineering, Michigan State University, East Lansing, MI 48824, USA
[5] School of Physics & Astronomy, University of Minnesota, Twin Cities, Minneapolis, MN 55455, USA
[6] Lawrence Livermore National Laboratory, P.O. Box 808, L-414 Livermore, CA 94550, USA
[7] Department of Physics, University of Basel, 4056 Basel, Switzerland
[8] Department of Physics, University of Notre Dame, Notre Dame, IN 46556, USA
Received 2009 November 23; accepted 2010 May 12; published 2010 June 30

ABSTRACT

We present results from the JINA REACLIB project, an ongoing effort to maintain a current and accurate library of thermonuclear reaction rates for astrophysical applications. Ongoing updates are transparently documented and version tracked, and any set of rates is publicly available and can be downloaded via a Web interface at http://groups.nscl.msu.edu/jina/reaclib/db/. We discuss here our library V1.0, a snapshot of recommended rates for stable and explosive hydrogen and helium burning. We show that the updated reaction rates lead to modest but significant changes in full network, one-dimensional X-ray burst model calculations, compared with calculations with previously used reaction rate sets. The late time behavior of X-ray burst light curves shows significant changes, suggesting that the previously found small discrepancies between model calculations and observations may be solved with a better understanding of the nuclear input. Our X-ray burst model calculations are intended to serve as a benchmark for future model comparisons and sensitivity studies, as the complete underlying nuclear physics is fully documented and publicly available.

Key words: nuclear reactions, nucleosynthesis, abundances – X-rays: bursts

Online-only material: color figures

1. INTRODUCTION

Nuclear astrophysics addresses questions related to the origin and evolution of the chemical elements, as well as astrophysical events powered by nuclear processes. Pioneering efforts identified and disentangled many of the nuclear processes needed to explain observations (Burbidge et al. 1957; Cameron 1957; Wagoner 1969; Howard et al. 1971; Audouze et al. 1973) and many more have been discovered since (see Clayton 1968; Wallace & Woosley 1981; Rolfs & Rodney 1988; Woosley et al. 1990; Woosley & Hoffman 1992; Pagel 1997; Wallerstein et al. 1997; Schatz et al. 1998; Iliadis 2007; Boyd 2008; Fröhlich et al. 2006; Pruet et al. 2006 for recent reviews). Key to this exploration is reliable and up-to-date nuclear physics input. Of foremost importance in most astrophysical scenarios are thermonuclear reaction rates. These needs drove many efforts into the systematization and formulation of reaction rate compilations which have played a central role in the field early on (Fowler et al. 1967, 1975; Harris et al. 1983; Caughlan et al. 1985; Caughlan & Fowler 1988). Here we focus on charged particle reactions of relevance in hydrogen and helium burning scenarios in stars, core collapse supernovae, novae, and X-ray bursts. Caughlan & Fowler (1988) were the last of a series of widely used compilations summarizing mostly charged particle reaction rates on stable targets taking into account experimental and theoretical nuclear physics information. An updated compilation of similar scope was presented by the NACRE collaboration (Angulo et al. 1999) focusing exclusively on charged particle-induced reaction rates on mainly stable targets in the $A = 1$–28 mass range. Triggered by the advances of radioactive beam experiments over the last few decades, efforts to make reaction libraries complete for explosive hydrogen burning scenarios resulted in compilations relevant for novae (Wiescher et al. 1986) and the *rp*-process in X-ray bursts (van Wormer et al. 1994; Schatz et al. 1998). Iliadis et al. (2001) more recently presented a compilation of proton capture reaction rates in the $A = 20$–40 mass range that included all relevant reactions on neutron deficient radioactive targets, including theoretical reaction rates. Neutron capture reactions have also been extensively compiled (Allen et al. 1971; Bao & Käppeler 1987; Beer et al. 1992; Bao et al. 2000). The KADoNiS project (Dillmann et al. 2006) has combined these neutron capture rate evaluations, supplemented with more recent experiments and provided easy Web-access to their database[10]. These compilations are complemented by large data sets of theoretical rate calculations based on shell model (Herndl & Brown 1997; Fisker et al. 2001) or Hauser–Feshbach models (Hauser & Feshbach 1952; Holmes et al. 1976; Woosley et al. 1978; Woosley & Hoffman 1992; Rauscher & Thielemann 1998, 2000; Rauscher 2008a; Goriely 1998; Arnould & Goriely 2003).

However, compilations only cover a small subset of the types of rates and mass ranges needed in modern nuclear reaction network calculations. This has led astrophysical modelers to compile their own complete set of rates making it difficult to

[9] Corresponding author: cyburt@nscl.msu.edu

[10] http://www.kadonis.org

compare model calculations by different groups and to identify reaction rates that have been used in specific calculations. Another problem is that compilations are typically frozen at some cutoff date prior to the time of publication, often as a one-time project or with very long publication intervals. Because of this, new experimental or theoretical results are often not taken into account in astrophysical models. To address these problems, we present here a new public database for thermonuclear reaction rates maintained by the Joint Institute for Nuclear Astrophysics, the JINA REACLIB database. It is based on an updated version of Thielemann's REACLIB reaction rate library that has been used by various groups over the last decades (Thielemann et al. 1987; Wiescher et al. 1986; van Wormer et al. 1994; Schatz et al. 1998). It represents a reaction rate compilation that is continuously updated yet provides well-defined snapshots at regular intervals to allow comparison of model calculations by different groups. The main criterion for updates is to provide the best possible choice of reaction rates based on what is available in the literature at any given time. Data on reaction rates that require a thorough evaluation of previous work are only included once such an evaluation has been published. Reaction rates are presented in an analytic form, and fit within 5% of literature values unless otherwise noted. Version tracking allows users to document and reference a specific reaction rate set used in a calculation, which can then be looked up in the database. This is done through a Web-interface system, where users can access the database[11].

Our database is complementary to the BRUSLIB database and NETGEN reaction network generator Web interface[12], which is also an effort to maintain complete reaction libraries (Aikawa et al. 2005). BRUSLIB contains experimental-based rates from the NACRE collaboration (Angulo et al. 1999), Iliadis et al. (2001) and Bao et al. (2000), and has been further supplemented with other experimental- and theory-based thermonuclear and weak reaction rates last updated in 2005 November (See Aikawa et al. 2005 for details). Instead of the parameterized REACLIB format, BRUSLIB presents data in tabular form and includes estimates for rate uncertainties from the NACRE collaboration.

The REACLIB release presented here focuses on reaction rates needed to model hydrogen and helium burning environments. A particular goal of this release was to improve models of Type-I X-ray bursts (Schatz & Rehm 2006; Strohmayer & Bildsten 2006). After their discovery (Grindlay 1976; Evans et al. 1976), X-ray bursts were soon explained as resulting from unstable hydrogen and helium burning in material on the surface layers of neutron stars accreted from a companion star (Hansen & van Horn 1975; Woosley & Taam 1976; Joss 1977). X-ray bursts release about 10^{39}–10^{40} erg in 10–100 s and exhibit recurrence times of hours to days. With over 70 known sources they are the most frequent thermonuclear explosions observed in the Galaxy. Current X-ray observatories have accumulated a vast body of detailed observational data. These have revealed and reinforced many puzzles and open questions such as bursts with multiple peaks (Hoffman et al. 1980; Sztajno et al. 1985; van Paradijs et al. 1986; Watts & Maurer 2007), the unexplained burst behavior at high accretion rates (Kuulkers et al. 2002; Cornelisse et al. 2003), or the origin of ^{12}C in the burst ashes thought to be required to power the rarely observed superbursts (Cumming & Bildsten 2001; Strohmayer & Brown 2002). Improved nuclear data are needed to clarify whether these issues reflect problems in the nuclear physics input or require advances in astrophysical modeling. Improved nuclear physics is also needed to extract system parameters such as accreted hydrogen content, accretion rate, or neutron star properties from detailed comparisons of model bursts with observations, and to predict possible spectral signatures from ejected ashes that could be targets of current and future X-ray observatories (Weinberg et al. 2006). Despite the problems of current burst models to explain certain observational features, in some cases overall good agreement between burst calculations and observations has been found (Heger et al. 2007), though some discrepancies remain. However, sensitivity studies have demonstrated that burst light curves do vary significantly within nuclear physics uncertainties (Woosley et al. 2004; Parikh et al. 2008), leaving the possibility that such agreement is fortuitous with deficiencies in the nuclear physics compensating for deficiencies in the astrophysical models or the chosen model parameters.

The principal nuclear reaction sequences in X-ray bursts have recently been delineated in detail by Fisker et al. (2008). These are characterized by ignition driven by the 3α reaction and rapid breakout from the CNO cycles, followed by helium burning via the αp-process and hydrogen burning via the rp-process ending under the most favorable conditions (high hydrogen contents in the accreted matter, low metallicity, and high accretion rate) in a SnSbTe cycle (Schatz et al. 2001).

Our work presented here includes an update of the relevant reaction rates of 3α, (α,p), (α,γ), and (p,γ) reactions from H to Te using newly published reaction rates based on experimental results. We also present new rules for fitting reaction rates that avoid problems that were present in REACLIB in the past, such as charged particle reaction rates that become non-physical at low temperatures. Weak interaction decay rates that do not depend on density are also updated and included. In addition, we present a new set of theoretical reaction rates calculated with the code NON-SMOKER$^{\rm WEB}$ v5.0w and use updated nuclear masses that take into account new experimental information from mass measurements and nuclear lifetime constraints. In Section 2, we discuss how reaction rates are updated and verified in the REACLIB database. In Section 3, we discuss the new content of the database. We then use in Section 4 a state of the art multi-zone X-ray burst model (Woosley et al. 2004) to calculate a sequence of X-ray bursts with the updated reaction library. The importance of these calculations is two fold. First, using updated reaction rates leads to more reliable calculations that either validate or falsify conclusions based on earlier model calculations. Second, to our knowledge the calculation presented here is the first full one-dimensional X-ray burst simulation with fully documented and publicly available nuclear physics input. It is intended to serve as a benchmark and starting point to compare different burst models from various groups, and to determine the impact of future improvements in the nuclear physics. We conclude our results and discuss future prospects for this research in Section 5.

2. THE JINA REACLIB DATABASE

The JINA REACLIB database is completely public and accessible to the community via the World Wide Web. The interface[11] is PHP-driven[13] and connected to a MySQL database[14]. The current version of the database stores reaction rates as a function of temperature in the seven-parameter rate parameterization of

[11] http://groups.nscl.msu.edu/jina/reaclib/db/
[12] http://www-astro.ulb.ac.be/Netgen
[13] http://www.php.net
[14] http://www.mysql.com

Thielemann et al. (1987) and F.-K. Thielemann (1995, private communication):

$$\lambda = \exp\left[a_0 + \sum_{i=1}^{5} a_i T_9^{\frac{2i-5}{3}} + a_6 \ln T_9\right]. \quad (1)$$

These rates go into a set of stiff coupled differential equations, and are then evolved to solve the abundance changes of the nuclides in the network. For a single reaction channel ($A + B \rightarrow C + D$), the equations take the form

$$-\frac{1}{\mathcal{N}_A}\partial_t Y_A = -\frac{1}{\mathcal{N}_B}\partial_t Y_B = \frac{1}{\mathcal{N}_C}\partial_t Y_C = \frac{1}{\mathcal{N}_D}\partial_t Y_D = \frac{Y_A^{\mathcal{N}_A}}{\mathcal{N}_A!}\frac{Y_B^{\mathcal{N}_B}}{\mathcal{N}_B!}\rho^{\nu}_{\rm baryon}\lambda, \quad (2)$$

where Y_i are the molar abundances per gram and $\mathcal{N}_i$ is the number of nuclides of type i produced or destroyed in the reaction and $\nu = \mathcal{N}_A + \mathcal{N}_B - 1$. By definition, the reaction rate or "rate of reaction" is given by the entire right-hand side of Equation (2), but the term reaction rate is used synonymously for the "reduced" reaction rate or reactivity, λ, throughout this paper and in the REACLIB database. For a network of reactions, each $\partial_t Y_i|_{A+B\rightarrow C+D}$ is summed over all participating reactions, including their reverse rates. For unary rates, $\lambda = 1/\tau$ has units of s^{-1}, inversely proportional to the mean lifetime. For binary rates, $\lambda = N_A<\sigma v>$ has units of $cm^3\ s^{-1}\ mol^{-1}$, while for trinary rates, λ has units of $cm^6\ s^{-1}\ mol^{-2}$. Multiple sets of parameters can be added to fit more complex temperature dependencies.

Reaction rates are continuously updated to ensure that the latest progress in nuclear physics is available to address astrophysical problems. Rather than delete old rates as they are supplanted by newer evaluations, we keep them in the database under different version numbers. While only one version is recommended, this gives users a choice. A rate detail page allows detailed comparison between different reaction rate versions in tabular and graphical forms.

In some cases it might be desirable to carry out an astrophysical model calculation with a well-known set of rates that, for example, is being used by other groups. This allows one to compare results from different models in a meaningful way. To address this need, we release on a regular basis snapshots of the currently recommended rates. The reaction rates discussed in this paper are such a snapshot called REACLIB V1.0. Users can also create their own snapshots and store them in the system. Snapshots can be referenced in publications, and can be accessed through the Web interface so that readers can look up reaction rates used in a particular study, or can download the same set of reaction rates for their own calculations.

Reaction rate updates are considered as rates appear in the literature or are suggested by users. This process is documented on the database Web site, and a complete history of updates is available[15]. In addition, documents created in the process of evaluating a reaction rate are stored in the database as well. Possible new rate entries are found from several sources. (1) Rates can be recommended by the community as new experimental/theoretical work is completed (published). This can be done via our Web interface or by direct communication. (2) Papers with relevant reaction rate information in the JINA Virtual Journal of Nuclear Astrophysics[16] (VJ), a weekly compilation of new publications in nuclear astrophysics, are flagged by the editor, and information is transferred through Web-based tools into the update process for the REACLIB database. (3) Rates can also be submitted and evaluated at the http://www.nucastrodata.org repository, in development at ORNL (Smith et al. 2008).

The main motivation for updating our database is to provide the best reaction rates available in the literature at any given time. Relevant reaction rate information is collected on a regular basis for each reaction rate, compared with previously published information, and then subjected to an initial screening process. The possible outcomes of this screening process are a recommendation to either (1) enter the published reaction rate directly into the database (*"Implement As Published"*), (2) store the information for a future detailed evaluation (*"Evaluation Needed"*), (3) ignore the information (*"No Action Needed"*). Immediate implementation is typically recommended when the published work is a thorough evaluation taking into account all previous work, or if it represents an obvious improvement compared with the previously available reaction rate. Examples for an obvious improvement include the replacement of theory with credible experimental data or a dramatically improved experiment. In most cases, these are reaction rates where very little previous experimental data are available. Storing the information for future evaluation is typically recommended for reaction rates where a lot of information is available that has to be taken into account in a consistent way and where the published work does not provide such a complete evaluation. Other cases include a conflict with previous work without a clear explanation or obvious improvement, or incomplete information that requires a major effort to extract a reaction rate. Once a published complete evaluation becomes available, the result is again considered for implementation into the database. Leaving a reaction rate out is recommended for cases where the information turns out to be not relevant for the astrophysical reaction rate, or if it results in no significant difference to previous work. The decisions are documented on the database Web site and can be discussed by the community through discussion threads.

New rates are fit to the standard seven-parameter REACLIB form given in Equation (1). This format is capable of handling all reaction types. Multiple sets of Equation (1) with differing parameters, a_0 through a_6, can be summed in order to properly fit rates with numerous resonant and non-resonant contributions. Non-physical behavior of the reaction rates outside of the fitted temperature range is avoided by enforcing physical constraints on the parameters (Wagoner 1969; Woosley et al. 1978). The enforcement of physical constraints on the fit parameters is an improvement brought to the REACLIB database with the V1.0 update. Unique rules exist for assigning values to the rate parameters a_0–a_6 in the cases of charge-induced non-resonant, neutron-induced non-resonant, and narrow resonant rate contributions. In practice, these rules should serve more as guidelines so that actual parameter values used are within proximity to those theoretically assigned. For positive Q-value reactions these are summarized in Table 1.

In Table 1 N_A is Avogadro's number, σ is the cross section in cm^2, v is the center of mass relative speed in cm s^{-1}, E is the center of mass relative energy in MeV, Z_1 and Z_2 are the target and reactant charges, A is the reduced mass of the reactants in atomic mass units, $S(0)$ is the astrophysical S-factor

[15] http://groups.nscl.msu.edu/jina/reaclib/db/status.php

[16] http://groups.nscl.msu.edu/jina/journals/jinavj/

Table 1
Shown are the Fitting Rules for Various Types of Reaction Rates, Including Non-resonant (NR) Charge-induced (q-induced) and n-induced Reactions, as well as Narrow Resonant Reactions

q-induced NR	n-induced NR	Narrow Resonant
$a_0 = \ln[B(\frac{Z_1 Z_2}{A})^{\frac{1}{3}} S(0)]$	$a_0 = \ln(N_A C^{\ell} \frac{\Gamma(\ell+3/2)}{\Gamma(3/2)} (\frac{\sigma v}{E^{\ell}})_{E=0})$	$a_0 = \ln(DA^{-3/2}\omega\gamma)$
$a_1 = 0$	$a_1 = 0$	$a_1 = -11.6045 E_r$
$a_2 = -4.2486(Z_1^2 Z_2^2 A)^{\frac{1}{3}}$	$a_2 = 0$	$a_2 = 0$
$a_3 =$ float	$a_3 =$ float	$a_3 = 0$
$a_4 =$ float	$a_4 =$ float	$a_4 = 0$
$a_5 =$ float	$a_5 =$ float	$a_5 = 0$
$a_6 = -2/3$	$a_6 = \ell$	$a_6 = -3/2$

Notes. These rules enforce the proper low-temperature analytics. All parameters with numerical values can be fixed, and those specified as "float" can be varied to accommodate the rate changes at higher temperature.

in MeV-barn at zero energy, ℓ is the minimum orbital angular momentum value in units of $\hbar$, $\Gamma(z)$ is the Gamma function, $\omega\gamma$ is the narrow resonance strength in MeV, E_r is the narrow resonance energy in MeV, $B = 7.8318 \times 10^9$ cm^3 s^{-1} mole^{-1} MeV^{-1} barn^{-1}, $C = 0.08617$ MeV, and $D = 1.5394 \times 10^{11}$ cm^3 s^{-1} mole^{-1} MeV^{-1}. Reaction rates from shell model or statistical model calculations with high level densities should follow the non-resonant prescriptions. If a rate is comprised of both non-resonant and resonant pieces, multiple sets of the seven-parameter fits may be used to describe the rate. It may also be necessary to fit multiple sets to obtain the requisite precision. Proper use of REACLIB form and fitting procedure should yield a reaction rate fit that is within 5% of the data. 5% fit accuracy is adhered to in the database and is considered acceptable by the authors who note that experimental error is rarely better than 10%–15% and theoretical errors are often more than 30%. It may occur that a fit to 5% precision is not possible. Such cases are listed on an automatically generated deviations list and an effort is made to constantly improve such cases. Future updates may include adding two more terms in each exponential set (i.e., $T_9^{\frac{7}{3}}$ and T_9^3 terms) to improve fitting performance and fit precision.

Once a rate is fitted it will be entered into the database as a "Future" rate, which is not visible as part of the database. The rate is then independently verified to ensure quality control, and actual rate values are entered into a verification database that is run automatically on a regular basis displaying any unacceptable discrepancies (more than 5%) on the Web site. This documents cases of inaccurate fits and ensures the integrity of the database over time. Once this process is completed, the rate will become available in the database. In some cases the new rate might not become the recommended rate version, but will be made available as a choice.

3. NEW REACLIB CONTENT

Our library has been updated using available information from experiments (e.g., cross sections, resonance strengths, etc.) as well as theoretical rate predictions. The bulk of the rates are from new statistical model calculations with a recently updated version of NON-SMOKER$^{\rm WEB}$ (see Section 3.3) using updated nuclear masses (see Section 3.2). In the *sd*- and *fp*-shell, shell model based reaction rates are used where available (see Section 3.3). These theoretical rates are replaced with experimentally based reaction rates for the relatively small number of cases where these are available (see Section 3.1). In addition, several reaction rates that were taken over from older REACLIB versions were refitted to avoid unphysical behavior.

3.1. Experiment-based Rates

Many of the experiment-based reaction rates were taken from the compilations of the NACRE collaboration (Angulo et al. 1999) and from Iliadis et al. (2001) for stable and unstable nuclei respectively. In some cases other reaction rates have been chosen, mostly because more recent experimental information became available. These cases are discussed in the following. Stellar enhancement factors that take into account the population of excited states in the target nucleus when immersed in the astrophysical plasma, are taken from the relevant NON-SMOKER statistical model calculations (Rauscher & Thielemann 1998, 2000; Rauscher 2008a) except for ^{32}Cl(p,γ) where a stellar enhancement factor is given in the most recent evaluation of the rate by Schatz et al. (2005).

^{4}He($\alpha\alpha$, γ)^{12}C is a key reaction in several sites of nucleosynthesis. It is the reaction that triggers the thermonuclear runaway in X-ray bursts. In addition to the dominant contribution of the Hoyle state in ^{12}C, the NACRE compilation (Angulo et al. 1999) includes an extra contribution from a theoretically predicted 2^+ resonance at 9.1 MeV. New experimental data of the inverse process (^{12}C$^* \rightarrow 3\alpha$) have been obtained by Fynbo et al. (2005) providing new information on additional resonances beyond the Hoyle state. They find a number of interfering broad resonances, which they include in their compiled reaction rate, but conclude that the presence of a state at 9.1 MeV is unlikely based on their data. We therefore recommend the reaction rate by Fynbo et al. (2005). The differences between the Fynbo et al. (2005) and the NACRE rate (Angulo et al. 1999) are negligible for X-ray burst temperatures. Recently, after the cutoff date for this compilation, some evidence for a 2+ state at 9.6 MeV was found (Freer et al. 2009; Diget et al. 2009). If correct it would affect the rate at very high temperatures, though its impact will be lessened compared with the prediction of NACRE because of the higher energy of the state.

^{12}C(α, γ)^{16}O is a difficult reaction to measure at energies relevant for astrophysics. The reaction is important in hydrostatic and explosive helium burning regimes. Buchmann (1996) and Kunz et al. (2002) used an R-matrix formalism that combines information about ^{16}O structure, ^{12}C-α scattering, as well as direct capture measurements available at the time to derive the low energy behavior of this cross section. Since then, significant experimental progress has been made (Kunz et al. 2001; Schürmann et al. 2005a, 2005b; Tang et al. 2007, 2008). Kunz et al. (2001) determine the angular distributions of γ rays from the direct reaction at 20 energies from 0.95 to 2.8 MeV. These data can be used to determine the E1 and E2 components of the S-factor separately. Tang et al. (2007, 2008) measure the

β-delayed α decay of ^{16}N, extracting constraints on the E1 component of the S-factor at 300 keV. New data from Schürmann et al. (2005a, 2005b) measure the total ^{12}C$(\alpha,\gamma)^{16}$O cross section at energies between 1.9 and 4.9 MeV in inverse kinematics via use of the ERNA recoil separator. However, as discussed for example in Buchmann (2008), the total S-factor obtained in more recent evaluations agrees well with the value obtained by Buchmann (1996). We therefore continue to recommend the Buchmann (1996) rate.

^{13}N$(p,\gamma)^{14}$O is an important reaction in the hot CNO cycle. It has undergone several experimental updates since the NACRE collaboration's recommendation (Angulo et al. 1999). Tang et al. (2004) use the peripheral reaction ^{14}N(^{13}N,^{14}O)^{13}C to extract an asymptotic normalization constant (ANC) for $^{14}\mathrm{O}\rightarrow{}^{13}\mathrm{N}+p$. This ANC is then used to calculate the direct capture component of this cross section. The rate is dominated by a low energy resonance at $E_R = 528$ keV. Tang et al. (2004) infer that this state interferes with the direct capture component enhancing the low energy cross section. More recently Li et al. (2006) have re-examined this reaction by similarly measuring the ANC, but through the reaction ^{13}N$(p,\gamma)^{14}$O. They confirm the results from Tang et al. (2004). We therefore adopt the most recent Li et al. (2006) results as our recommended value.

The ^{14}N$(p,\gamma)^{15}$O reaction is the slowest reaction in the low temperature CNO cycle. Recently, a number of new direct measurements have been performed (Imbriani et al. 2005; Runkle et al. 2005) that have extended the measured cross sections to significantly lower energies. Both groups evaluate the available data and obtain comparable S-factors, so we chose to implement Imbriani et al. (2005). The new reaction rate is significantly lower at low temperatures compared with the rate given in NACRE (Angulo et al. 1999) and Caughlan & Fowler (1988), but agrees well with previous compilations for $0.2 < T_9 < 2$. More recently, the LUNA Collaboration et al. (2006) measured the total cross section down to 70 keV. In addition, Marta et al. (2008) have explored the critical issue of the interference between the 259 keV resonance and direct capture component and provide a stringent limit for the extrapolation to lower energies. However, a comprehensive evaluation that would allow us to include the new data in our database was not available at the cutoff date for this work.

^{14}N$(\alpha,\gamma)^{18}$F is important in early phases of He burning, taking place before the triple-α reaction. It is also the main source of ^{22}Ne, via another α capture, which is a neutron source for the s-process (^{22}Ne$(\alpha,n)^{25}$Mg). Görres et al. (2000) have recently measured the lowest lying resonance properties and the direct capture into the ground state. This yields changes in the adopted rate of factors of 2–5 compared with Caughlan & Fowler (1988) and NACRE (Angulo et al. 1999) in the astrophysical temperature range of interest $0.1 < T_9 < 0.5$.

^{15}N$(\alpha,\gamma)^{19}F$ is a possible source of ^{19}F in Asymptotic Giant Branch stars. Recent experimental efforts by Wilmes et al. (2002) have measured the resonance properties of several states in ^{19}F. Besides observing two levels for the first time, they were also able to identify two levels as α-cluster states. The resulting thermonuclear reaction rate is identical to NACRE (Angulo et al. 1999), though with reduced uncertainties. Wilmes et al. (2002) is recommended in the REACLIB database.

The reaction ^{14}O$(\alpha,p)^{17}$F is important in the hot CNO cycle. It bypasses ^{14}O β-decay for $T_9 > 0.35$. Hahn et al. (1996) evaluated this reaction rate, tabulating two rates differing only in the sign of the assumed interference between the non-resonant and $E = 6.25$ MeV resonance. We have adopted the constructive interference rate as our recommended value. The two rates agree at temperatures beyond $T_9 \sim 0.5$, but are an order of magnitude different at lower temperatures. Recent measurements suggest that the rate adopting the constructive interference is accurate to within 50% (J. C. Blackmon 2009, private communication).

^{15}O$(\alpha,\gamma)^{19}$Ne is an important hot-CNO breakout reaction for novae and X-ray bursts, competing with ^{18}Ne$(\alpha,p)^{21}$Na. The dominant uncertainty stems from the α-width of a resonance at $E_X = 4033$ keV. The α branching ratio B_α is strongly Coulomb suppressed, since it is only 500 keV above threshold. Previous analyses have estimated its strength using iso-spin symmetry (Mao et al. 1995). An experimental upper limit was placed by Davids et al. (2003), $B_\alpha < 4.3\times10^{-4}$ at 90% confidence. Tan et al. (2007) find $B_\alpha = (2.9\pm2.1)\times10^{-4}$, which would yield a 90% confidence upper limit of $B_\alpha < 5.6\times10^{-4}$ if errors were normally distributed. We adopt the thermonuclear reaction rate calculated in Mao et al. (1995) and tabulated in Hahn et al. (1996), which finds $B_\alpha \approx 1.2\times10^{-4}$. Rates from Caughlan & Fowler (1988), Hahn et al. (1996), and Fisker et al. (2007) are within ~50% of each other at breakout temperatures ($T_9 \sim 0.4$–0.6).

^{17}O$(p,\gamma)^{18}$F and ^{17}O$(p,\alpha)^{14}$N are important in hydrogen burning nucleosynthesis, and compete against each other in the CNO cycle. Recently, both Fox et al. (2005) and Chafa et al. (2007) measured resonance properties in the ^{18}F system. They observed previously unobserved states important for the low energy nuclear cross section. Fox et al. (2005) estimated the direct capture components using a potential model, opting to ignore the low energy data, due to issues with resonance subtraction. Chafa et al. (2007) perform this subtraction and find agreement with the shape of the direct capture, though with a higher value, to match the data. These differences are washed out by the large uncertainties assigned to this component. For the resonant contribution to the reaction rate, a new resonance at $E_R = 183.3$ keV plays an important role. For (p,α), the resonance strengths given by Fox et al. (2005) and Chafa et al. (2007) agree and have been confirmed in a new experiment by Moazen et al. (2007). The resulting (p,α) reaction rate agrees with NACRE (Angulo et al. 1999) within a factor of 2 from $0.5 < T_9 < 2$. The largest deviation of a factor of 20 is at $T_9 = 0.2$ because of the new resonance. For (p,γ), the resonance strengths obtained by Fox et al. (2005) and Chafa et al. (2007) disagree however by almost a factor of 2 (more than one standard deviation). The resulting (p,γ) rates are within 40% of each other for $T_9 < 0.5$ and within 10% from $0.5 < T_9 < 5$. As no detailed evaluation of this situation is available in the literature, we for now adopt the (p,γ) and (p,α) rates by Chafa et al. (2007).

^{17}F(p,γ)^{18}Ne is an important reaction in the hot CNO cycle, dominating over ^{17}F β-decay when $T_9 > 0.093$. The recommended rate is that by Bardayan et al. (2000). The new theory calculation by Dufour & Descouvemont (2004) agrees quite well with Bardayan et al. (2000).

^{18}Ne$(\alpha,p)^{21}$Na is a hot CNO cycle breakout reaction, competing with ^{15}O$(\alpha,\gamma)^{19}$Ne. We adopt a rate based on two compilations: at low temperature we use Görres et al. (1995), while at high temperature we use Bradfield-Smith et al. (1999). New constraints come from experiments by Chen et al. (2001) and Chae et al. (2009), populating states in ^{22}Mg via the ^{12}C(^{16}O,^{6}He)^{22}Mg and ^{24}Mg(p,t)^{22}Mg reactions, respectively. The rates determined from Chen et al. (2001) and Chae et al. (2009) agree quite well with each other and within a factor of 4 of the combined Görres et al. (1995) and Bradfield-Smith

et al. (1999) rate. However, inclusion of these new results will require a comprehensive rate evaluation, which is currently not available in the literature.

^{21}Na(p, γ)^{22}Mg acts as a pathway reaction, linking the CNO cycle and breakout reactions with those of the αp and rp processes. Recently the strengths of the relevant resonances have been measured directly for the first time (D'Auria et al. 2004) leading to a factor of 10 change at $T_9 = 1$ from the Bateman et al. (2001) reaction rate tabulated in Iliadis et al. (2001). We therefore recommend the new evaluated reaction rate given by D'Auria et al. (2004).

^{22}Na(p, γ)^{23}Mg is a rapid-proton capture occurring early in the rp-process. We adopt the NACRE (Angulo et al. 1999) rate. New data from Jenkins et al. (2004) have been sorted into REACLIB's "to be evaluated" list, while Comisel et al. (2007) has been sorted into REACLIB's "no action needed" list. They present new upper and lower limits, but adopt NACRE's central rate.

^{22}Mg(p, γ)^{23}Al is another rapid-proton capture reaction occurring early in the rp-process. We adopt the rate by Caggiano et al. (2001), tabulated in Iliadis et al. (2001). The Coulomb dissociation measurement of this reaction by Gomi et al. (2005) does not present enough information for creating a reaction rate.

^{23}Na(p, γ)^{24}Mg and ^{23}Na(p, α)^{20}Ne are important reactions that are key to understanding the NeNa cycle. These reactions compete against each other, either maintaining the cycle or driving the flow out of the cycle. There are several low energy resonances in ^{24}Mg just above the ^{23}Na+p threshold that greatly influence these reaction cross sections. Hale et al. (2004) populated these states in ^{24}Mg via the ^{23}Na(^{3}He,d)^{24}Mg reaction, obtaining better constraints on spectroscopic factors. Both Hale rates, which we adopt here, agree with Caughlan & Fowler (1988) and NACRE (Angulo et al. 1999) within $\sim$20% between $0.2 < T_9 < 3$. The main difference is due to a previously unobserved resonance at $E_R = 138$ keV.

^{25}Al(p, γ)^{26}Si is an important reaction for ^{26}Al production; it provides a channel that avoids the population of the ^{26}Al ground state. Its 1.8 MeV decay γ-rays, which can be observed with current γ-ray observatories, can offer powerful constraints of models of ^{26}Al production. This reaction is studied via indirect techniques, generally using theory calculations to extract relevant p and γ widths. Parpottas et al. (2004, 2006) claim a misassigned spin resulting in a deviation from previous works. Also, they claim that multi-step processes may be important in the extraction of level properties. Bardayan et al. (2006) explore this possibility further looking at smaller angles and show that is to some extent true, though Parpottas et al. (2004, 2006) overestimated the strength of the resonance at $E_R = 428$ keV. Otherwise, the resulting astrophysical reaction rates agree well in temperature ranges relevant for novae and X-ray bursts. We recommend the Bardayan et al. (2006) rate.

The ^{26}Si(p, γ)^{27}P reaction lies along the nucleosynthesis path of the rp-process. As the previous reaction, it is important in the flow bypassing the production of ^{26}Al in its ground state. The direct capture into the ground state has not been measured. Guo et al. (2006) determine the ANC of the mirror nucleus (^{26}Mg+n), and via mirror symmetry an ANC for ^{26}Si+p was extracted to calculate the direct capture cross section. Using excitation energies and Q-value measurements from recent work, they derive an astrophysical reaction rate. The rate agrees with Caggiano et al. (2001), tabulated in Iliadis et al. (2001) over the range $0.1 < T_9 < 2$. At lower temperatures the rates differ because of a factor of $\sim$2 difference in the direct capture components. Therefore, we adopt the rate from Guo et al. (2006).

The ^{30}P(p, γ)^{31}S reaction is important in explosive hydrogen burning scenarios such as novae and X-ray bursts. Cross-section estimates from statistical Hauser–Feshbach theory have been used in the past (Rauscher & Thielemann 2000) as discussed in Iliadis et al. (2001). Two recent experimental studies have identified one new level in ^{31}S (Jenkins et al. 2006) and remeasured many of the previously known ones (Jenkins et al. 2006; Ma et al. 2007). Both studies used the known levels in ^{31}S, together with estimates for spectroscopic factors and γ-widths, to calculate a new reaction rate based on individual resonances. Their results agree well, and we use here the rate from Jenkins et al. (2006).

The ^{32}Cl(p, γ)^{33}Ar reaction rate was previously based on sd-shell model calculations (Herndl et al. 1995). Clement et al. (2004) measured the excitation energies of the most important states in ^{33}Ar Clement et al. (2004). Using these data, Schatz et al. (2005) present a much more reliable reaction rate, that also takes advantage of an improved shell model interaction for estimates of spectroscopic factors, and that is adopted here. Unlike previous rate calculations, this new rate also takes into account the influence of the low-lying first excited state in ^{32}Cl, which leads to a stellar enhancement factor of up to a factor of 5 compared with the ground-state capture rate.

^{56}Ni(p, γ)^{57}Cu is the first rapid-proton capture reaction to happen after crossing the "most-tightly bound" threshold. It demarks the point in the rp-process where the rate of energy generation, and thus X-ray burst luminosity profiles, start to drop. We adopt the rate by Forstner et al. (2001), which is based on measurements of the n+^{56}Ni mirror spectroscopic factors (Rehm et al. 1998) and level information from Zhou et al. (1996).

3.2. New Masses

Q-values are among the most important input parameters for rp-process calculations, in particular at the high temperatures and proton densities reached in X-ray bursts where the path of the process is close to the proton drip line (its location depends on the Q-values and is determined mainly by local (p,γ)–(γ,p) equilibria (see Schatz et al. 1998; Schatz 2006). Reliable masses are also needed to calculate the theoretical reaction rates, that make up most of the reaction network needed to model X-ray bursts. Owing to major progress in mass measurements at rare isotope facilities many of the nuclear masses along the path of the rp-process are now known experimentally, albeit not always with sufficient precision. The remaining masses can be predicted either through the extrapolations by Wapstra et al. (2003), Audi et al. (2003b), or beyond the $N = Z$ line via Coulomb-shift calculations (Brown et al. 2002). Therefore, rp-process calculations in X-ray bursts no longer depend on global mass models. For the experimental nuclear masses we mostly use the 2003 Atomic Mass Evaluation (Wapstra et al. 2003; Audi et al. 2003b) (AME03, see exceptions below). We also updated these data with recent experimental results from ion trap mass measurements. Though it would be preferable to wait for a new mass evaluation, such measurements are typically of a precision that leads them to supersede previous data. The measurements included are the LEBIT measurements of ^{68}Se, ^{70}Br, ^{70}Se, ^{71}Br (Block et al. 2008), of ^{64,65}Ge, ^{66,67,68}As, ^{69}Se (Schury et al. 2007), and of ^{37,38}Ca (Ringle et al. 2007); the ISOLTRAP measurements in the Rb region (Kellerbauer et al. 2007) of $^{72-74}$Kr (Rodríguez et al. 2004); and the SHIPTRAP measurements in the Ag–Te region (Martın et al. 2007). The

LEBIT data on ^{68}Se are more than an order of magnitude more precise than the earlier CPT measurements (Clark et al. 2004). The ISOLTRAP data on $^{76-88}$Sr (Sikler et al. 2005) are very close to the data in AME03. At GSI's ESR the masses of *rp*-process nuclei ^{48}Mn, ^{44}V, ^{41}Ti, and ^{45}Cr have been measured. However, the data for ^{48}Mn and ^{45}Cr agree with AME03 with differences that are much smaller than the error bars. We therefore continue to use the AME03 data. For ^{44}V, the experimental error is quite large and we use the Coulomb shift extrapolation instead as discussed below. We also decided to implement the AME03 ^{41}Ti mass excess $\Delta = -15.700 \pm 0.1$ MeV despite of the significant difference to the experimental result ($\Delta = -15.090 \pm 0.360$ MeV) as this results in a proton separation energy for ^{42}V that is consistent with its non-observation (see below).

For the experimentally unknown masses of nuclei with $Z \leqslant N$ we adopt the AME03 extrapolations, except for ^{104}Sn, ^{112}Xe, and ^{113}Cs, where we adopt the revised extrapolations by Martın et al. (2007). These extrapolations have uncertainties that grow rapidly as one goes far from experimental-based masses. For nuclei beyond the $N = Z$ line, the Coulomb shift calculations by Brown et al. (2002) are an alternative. These calculations predict Coulomb mass shifts between mirror nuclei to typically 100 keV and have been shown to be more reliable than the AME03 extrapolations based on their smoother behavior (Brown et al. 2002). In particular, these Coulomb shifts allow much more reliable mass predictions for the critical nuclei (Schatz 2006) ^{65}As, ^{66}Se, ^{69}Br, ^{70}Kr, ^{73}Rb, and ^{74}Sr in connection with the recent high precision mass measurements of their mirrors using Penning traps. We adopt predicted masses from whichever method that yields the smaller uncertainty. In three cases, ^{44}V, ^{71}Kr, and ^{75}Sr, we also replace uncertain experimental data with more precise Coulomb shift extrapolations. In the case of ^{44}V and ^{75}Sr, the Coulomb shift value agrees within the errors with the experimental value. For ^{71}Kr the agreement is within 2σ but the experimental error is very large (650 keV).

In addition to mass measurements, there are a number of other experimental constraints on proton and α-separation energies. These are of particular importance as it is those separation energies that ultimately enter the reaction rate calculations, not the masses. These experimental constraints arise from lifetime limits obtained either by observation or non-observation of a particular isotope in a rare isotope beam experiment, or, in a few cases, by the measurement of particle energies of proton or α-decays. Such constraints are especially relevant here, as the location of the proton drip line has a strong influence on *rp*-process calculations. In the case of lifetime limits, we use a penetrability calculation to estimate a rough limit on the proton separation energy listed in Table 2 assuming a ground state to ground-state transition. In this simplified calculation, we set spectroscopic factors to unity and neglect deformation and any other details of the wave functions involved. Using a radius parameter of $r_0 = 1.11$ fm we were able to reproduce known proton energies for proton emitters ^{147}Tm, ^{151}Lu, ^{156}Ta, and ^{160}Re within 30 keV. We added this uncertainty to the limits listed in Table 2. We only consider odd Z nuclei. Because of the odd–even staggering of the proton drip line, the drip line for even Z isotopic chain extends far beyond the *rp*-process path and is not relevant here. Half-life limits are taken from the literature (see ENSDF for references, except for ^{50}Co and ^{55}Cu (Dossat et al. 2007), ^{81}Nb and ^{85}Tc (Janas et al. 1999), and ^{103}Sb (Lewitowicz et al. 1995)). In cases where a β-decay half-life is measured, we use the β-decay half-life as a rough lower limit for the proton decay partial half-life. We compare our updated mass table with these constraints. In most cases agreement was found, but in some instances we had to adjust masses. These are discussed in the following.

Table 2
Estimated Limits on Proton Separation Energies from Experimental Lifetime Limits

Isotope	Half-life	S_p (MeV)
^{42}V	< 55 ns	< -0.22
^{44}Mn	< 105 ns	< -0.25
^{45}Mn	< 70 ns	< -0.31
^{49}Co	< 35 ns	< -0.40
^{50}Co	> 39 ms	> -0.26
^{53}Cu	< 300 ns	< -0.31
^{54}Cu	< 75 ns	< -0.33
^{55}Cu	> 27 ms	> -0.24
^{60}Ga	> 70 ms	> -0.27
^{61}Ga	> 168 ms	> -0.27
^{64}As	> 40 ms	> -0.34
^{65}As	> 170 ms	> -0.29
^{68}Br	< 1500 ns	< -0.41
^{69}Br	< 24 ns	< -0.49
^{72}Rb	< 1200 ns	< -0.45
^{73}Rb	< 30 ns	< -0.54
^{76}Y	> 170 ns	> -0.58
^{77}Y	> 63 ms	> -0.41
^{81}Nb	< 44 ns	< -0.66
^{85}Tc	< 110 ns	< -0.69
^{89}Rh	> 1500 ns	> -0.91
^{93}Ag	> 1500 ns	> -0.97
^{103}Sb	> 1500 ns	> -0.89
^{104}Sb	> 470 ms	> -0.59

For ^{42}V, Borrel et al. (1992) report the non-observation requiring a proton separation energy of less than -0.218 MeV. With the new experimental ^{41}Ti mass from Stadelmann et al. (Stadlmann et al. 2004) one obtains a proton separation energy of 0.368 MeV. The new ^{41}Ti mass, however, deviates by 610 keV from the AME03 extrapolation of -15.7 ± 0.1 MeV. Given the large experimental uncertainty of 360 keV for ^{41}Ti, the much smaller mass uncertainty of ^{42}V (121 keV) and the fact that the AME03 extrapolation for the ^{41}Ti mass is estimated to be quite reliable (100 keV uncertainty) we decided to make the adjustment by using the extrapolated AME03 mass for ^{41}Ti. This results in a ^{42}V proton separation energy of -0.242 MeV consistent with its non-observation.

For ^{93}Ag, our mass table would predict a proton separation energy of -1.232 MeV inconsistent with its reported detection by Hencheck et al. (1994). However, as discussed in their paper this is only a tentative detection given the limited statistics and possible backgrounds. We therefore did not adjust the mass table for this case.

For ^{103}Sb, our mass table predicts a proton separation energy of -1.463 MeV inconsistent with the reported observation of this isotope by Rykaczewski et al. (1995). Evidence for ^{103}Sb was also reported by Smith et al. (2006), who find a significant β-branch. We estimate that the observation of ^{103}Sb requires a proton separation energy of at least -0.89 MeV, 0.58 MeV larger than predicted by AME03. As Figure 1 shows, other mass models are not able to predict the proton separation energies of Sb isotopes reliably, and all predictions are too small. We therefore adopted the limit of -0.89 MeV for the proton separation energy of ^{103}Sb. To obtain this separation energy, we adjusted both the ^{102}Sn and the ^{103}Sb mass, splitting

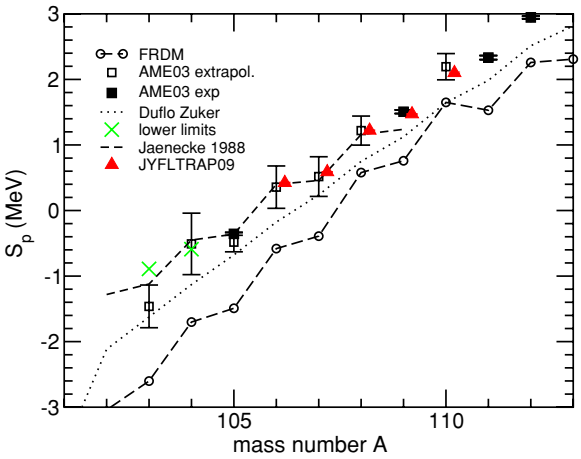

Figure 1. Proton separation energies (S_p) for neutron deficient Sb isotopes predicted by the FRDM mass model (Möller et al. 1995, dashed with circles), the AME 2003 extrapolations (Wapstra et al. 2003; Audi et al. 2003b, open squares), the mass model by Duflo & Zuker (1995), and the mass model by Jänecke & Masson (1988) together with experimental data from AME2003, updated with the recent determination of the proton separation energy of ^{103}Sb by Mazzocchi et al. (2007, solid squares). The lower limits obtained from the observation of ^{103}Sb and ^{104}Sb (see Table 2) are indicated by the green crosses. For comparison we also show the recent proton separation energies determined by Penning Trap mass measurements at JYFLTRAP and SHIPTRAP given in Elomaa et al. (2009), which have not been taken into account in this work yet (red triangles, error bars smaller than symbol size). They agree very well with the AME 2003 extrapolated values we used in our compilation.

(A color version of this figure is available in the online journal.)

the total necessary change in separation energy in proportion to each error bar. This changes the ^{102}Sn mass excess of -64.929 ± 0.131 by 0.175 MeV to -64.754 MeV and the ^{103}Sb mass excess of -56.178 ± 0.298 MeV by 0.401 MeV to -56.579 MeV.

As we would like to include at least one fast proton emitter in each odd Z mass chain in our reaction network we also added a mass excess value for ^{102}Sb of -50.61 MeV to the table taken from the mass model of Jänecke & Masson (1988), which does quite well in this mass region for short range extrapolations (see Figure 1). This value is highly uncertain. However, with the resulting very low proton separation energy of -1.6 MeV it is unlikely that this isotope plays a role in the *rp*-process reaction flow.

For ^{104}Sb, the predicted proton separation energy of -0.5 MeV is barely consistent with the observation of this isotope. However, the value is quite a bit smaller than the lower limit estimated by Mazzocchi et al. (2007) based on systematics, who even speculate that ^{104}Sb could be proton bound. This is another hint for a possible systematic underestimation of the proton separation energies of Sb isotopes near the proton drip line. More experimental data would be desirable to clarify this situation, which could have a significant impact on the *rp*-process reaction flow in the SnSbTe cycles (Schatz et al. 2001; Mazzocchi et al. 2007).

For ^{105}Sb, the recent detection of the α decay of ^{109}I together with the known α-decay energy of ^{108}Te and proton decay energy of ^{109}I allows for the determination of the ^{105}Sb proton separation energy of 0.356 ± 0.022 MeV (Mazzocchi et al. 2007). We used the new extrapolated mass excess of -71.668 ± 0.06 MeV for ^{104}Sn by Martın et al. (2007), which is motivated by nearby Penning trap mass measurements, as a basis, and adjusted the masses of ^{108}Te, ^{109}I, and ^{105}Sb using the measured α and proton separation energies. The resulting mass excesses are -65.798 ± 0.06 MeV for ^{108}Te, -57.680 ± 0.06 MeV for ^{109}I, and -64.023 ± 0.63 for ^{105}Sb.

The neutron deficient Te isotopes are known ground-state α-emitters. The known α energies are included in AME03 for ^{106}Te and higher. For ^{105}Te, a recent experiment detected the α-decay and determined an α-separation energy of -4.636 ± 0.006 MeV (Liddick et al. 2006). As the ^{105}Te mass is much more uncertain than the ^{101}Sn mass, we increased the ^{105}Te mass by 0.253 MeV (AME03 uncertainty 0.503 MeV) to adjust for this measurement. For ^{104}Te no experimental data are available. However, motivated by the new data on ^{105}Te, Mohr (2007) provides a theoretical estimate of the α-separation energy of -5.42 ± 0.07 MeV. Using the known ^{100}Sn mass in AME03 we obtain a ^{104}Te mass excess of -48.935 ± 0.7 MeV, which we added to our mass table.

Significant progress in mass measurements in the upper *rp*-process region has been achieved after the cutoff date for the present work (spring 2008). These will be considered in forthcoming REACLIB updates. However, given the significant increase in the body of precision data from Penning Traps, a new mass evaluation would be highly desirable before making such a comprehensive update.

3.3. New Theory Rates

Almost all the relevant proton- and α-induced reactions in X-ray bursts occur on unstable nuclei. Because of the experimental difficulties and limited rare isotope beam intensities at existing accelerator facilities, experimental information is sparse and the majority of the reaction rates in X-ray burst models are based on theoretical calculations. Closer to stability where level densities tend to be high, statistical model calculations using the Hauser–Feshbach method can be used. However, toward the drip line reaction Q-values tend to become small and the statistical model assumption of high level density might break down for some of the temperatures relevant for X-ray bursts (Rauscher et al. 1997). In addition, with fewer resonances contributing, and levels being spaced further apart, direct capture will also play a more important role (Rauscher (2008b, 2008c) and references therein). For the reactions furthest away from stability we therefore use shell model based reaction rates. In the *sd*-shell, we use the reaction rates by Herndl et al. (1995), which include estimates for individual resonances and a direct capture component calculated with a potential model. In the *fp*-shell up to $A \approx 64$, we use the shell model rates by Fisker et al. (2001). In cases where excitation energies are not constrained by experiments, shell model rates can have uncertainties of many orders of magnitude. Beyond $A \approx 64$, only Hauser–Feshbach rates are available. Therefore, in this mass range we use Hauser–Feshbach rates even in cases where level densities are not sufficient.

For the Hauser–Feshbach reaction rates we use a set labeled in the JINA REACLIB database with "ths8" calculated with the NON-SMOKER$^{\rm WEB}$ code version 5.0w (Rauscher 2008a). The Hauser–Feshbach code for astrophysical applications NON-SMOKER$^{\rm WEB}$ has been developed and used since 2004 and replaced the previous NON-SMOKER code (Rauscher & Thielemann 1998, 2000). This new code includes (apart from the web interface) several modifications, including improved numerical computation, updated nuclear properties (e.g., masses), and other model improvements[17]. Version 5.0w will also be the basis for the future multi-reaction mechanism code SMARAGD,

[17] For details, see the development history at http://nucastro.org.

currently under development (T. Rauscher 2010, in preparation). The final version of the new SMARAGD code will consider compound and direct reactions, will be able to follow individual γ transitions within a nucleus, and will allow the calculation of multi-particle emission, among several other additions and further improvements. The NON-SMOKER$^{\rm WEB}$ 5.0w code used here still stays close to the original NON-SMOKER code in the treatment of some of the nuclear properties required to calculate the cross sections and reaction rates but the internal modifications give rise to certain differences in the results, expected to yield improved predictions. Concerning the update of nuclear properties, of relevance here are mainly the inclusion of masses from Wapstra et al. (2003) and Audi et al. (2003b) with the additions described elsewhere in this work, updated experimental information on ground and excited state spins and parities from Nudat 2.4, National Nuclear Data Center[18], an improved prediction of ground-state properties when no experimental information is available, and a parity-dependent level density (Mocelj et al. 2007) to be used above the known experimental levels. The different spins and level densities as well as the parity treatment may lead to considerable changes in the predicted rates compared with the previous NON-SMOKER rates (Rauscher & Thielemann 2000). In case there is no experimental information from Nudat 2.4[18], the neutron and proton spins and parities from Möller et al. (1997) are used and coupled using Nordheim rules. There are a few cases at or beyond the dripline without entries in Möller et al. (1997). A simple assumption for the ground-state spin was made for these, setting it to $J^{\pi}_{\rm gs} = 3^{+}$ for odd–odd, $J^{\pi}_{\rm gs} = 0^{+}$ for even–even, and $J^{\pi}_{\rm gs} = 3/2^{+}$ for other nuclei. Reverse rates were calculated from rates for the reaction direction with positive Q-value using the reciprocity theorem of nuclear reactions and the standard assumption of detailed balance (see Blatt & Weisskopf 1991; Rauscher & Thielemann 2000; Kiss et al. 2008; Rauscher et al. 2009 for details).

The Hauser–Feshbach rates used here also do not include the direct capture reaction mechanism. These will be considered in the future SMARAGD code. However, given the uncertainties attached to currently predicted statistical model and direct capture rates far from stability, it is not unreasonable to still use pure Hauser–Feshbach rates without a direct component. This is because Hauser–Feshbach models tend to overestimate the rate when a considerable fraction of the total reaction flux should actually go into the direct channel. Including a direct component would lower the statistical contribution but keep the total reaction rate roughly the same at most interaction energies relevant to astrophysics (Goriely 1998; Descouvemont & Rauscher 2006).

3.4. Weak Rates

In the rp-process, (p, γ) reactions tend to be fast and therefore β^{+}-decays largely determine processing timescale and final abundance pattern. With the recent measurement of the half-life of ^{96}Cd (Bazin et al. 2008) all relevant nuclei have experimental ground-state half-lives. However, the stellar environment can significantly modify decay rates from their terrestrial values. As nuclei are fully ionized, the capture of bound electrons, which contributes to many of the terrestrial half-lives, is absent in the stellar environment of X-ray bursts. In addition, low-lying excited states can be significantly populated at the temperatures reached in X-ray bursts (kT ranges from 10–200 keV). It is well known that these states can have significantly different decay properties compared with the ground state, leading to differences between the stellar and terrestrial half-lives (Takahashi & Yokoi 1987). An example are the odd–odd $N = Z$ nuclei, which have ground states that decay by super-allowed Fermi transitions and very low lying states with significantly reduced decay rates. Continuum electron capture does not play an important role at the densities reached in X-ray bursts. To account for these effects we use in our burst model calculations the temperature- and density-dependent weak decay rates from Fuller et al. (1980, 1982a, 1982b, 1985) and Pruet & Fuller (2003). Currently these rates are not part of our REACLIB database, given their density dependence. Rather, our database includes updated terrestrial half-lives, both experimental (Audi et al. 2003a; Tuli & National Nuclear Data Center 2007) and theoretical (Möller et al. 2003), which can be used as a default, but are then superseded in the burst model with temperature- and density-dependent rates when available. The terrestrial decay rates in the database are separated into their respective partial decay rates, accounting for β-delayed particle emission, when such experimental data exist.

4. X-RAY BURSTS CALCULATIONS

The one-dimensional, multi-zone hydrodynamics code Kepler (Woosley et al. 2004) was used to simulate Type-I X-ray bursts using the latest snapshot version of the REACLIB database (REACLIB V1.0) to determine the impact the updated library has on this particular explosive burning scenario. The results using this library are compared to results obtained using the previous, proprietary reaction database (Kepler BDAT 9.1.1[19]) compiled specifically for use in Kepler. The model accretes solar metallicity material at a rate of $1.75 \times 10^{-9}\ M_{\odot}\ {\rm yr}^{-1}$, and is the same as the "A4" model in Heger et al. (2007). The neutron star is taken to be 10 km in radius with a mass of 1.4 $M_{\odot}$. This model differs slightly in accretion rate from model "A3" of that work, which showed very good agreement with observed light curves from the so-called "clocked burster," GS 1826-24.

Kepler couples the energy generation of a fully adaptive nuclear reaction network of up to 1300 isotopes to a one-dimensional thermodynamic simulation. It is thus able to consistently model the thermodynamic and compositional evolution of material through accretion and stable nuclear burning, to burst ignition (in this case from unstable 3α He burning), rp- and αp-process burning, and subsumption of the burst ashes beneath subsequent layers of accreted material, allowing the simulation of long sequences of X-ray bursts; while fully appreciating the underlying nuclear physics.

In order to investigate approximate steady-state bursting behavior, the first two bursts were removed from each sequence, since the accretion leading to the first burst tends to be rather unusual beginning on a bare ^{56}Ni surface and the second burst is affected directly by the atypical composition of the ashes from the first (compositional inertia). A difficulty is that even in an approximate steady state, after the third burst, some smaller burst to burst variations continue. This is also the case for observed bursts. Following previous work, for example Heger et al. (2007), we therefore analyze a sequence of $\sim$30 bursts and construct 1σ confidence bands for the burst light curve, which can then be compared for different calculations to judge the significance of light curve differences. Figure 2 shows these bands for the old reaction library used in Woosley et al. (2004) (Kepler BDAT) and our new updated REACLIB V1.0.

[18] http://www.nndc.bnl.gov/nudat2

[19] http://adg.llnl.gov/Research/RRSN

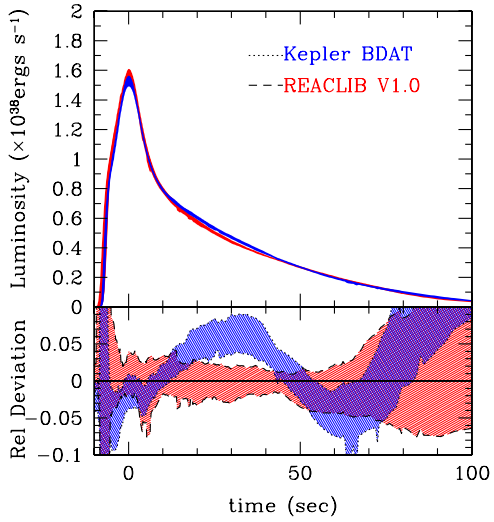

Figure 2. Simulated X-ray burst light curves generated using two different reaction rate libraries: the proprietary KEPLER BDAT rate library and REACLIB V1.0. The width of the bands gives the standard deviation of burst-to-burst variations. The horizontal dotted line on the upper plot indicates the accretion luminosity—not included in the model burst light curve—below which variations in burst luminosity are increasingly difficult to observe. The deviations in the lower pane are shown relative to the mean luminosity of the REACLIB V1.0 library light curves.

(A color version of this figure is available in the online journal.)

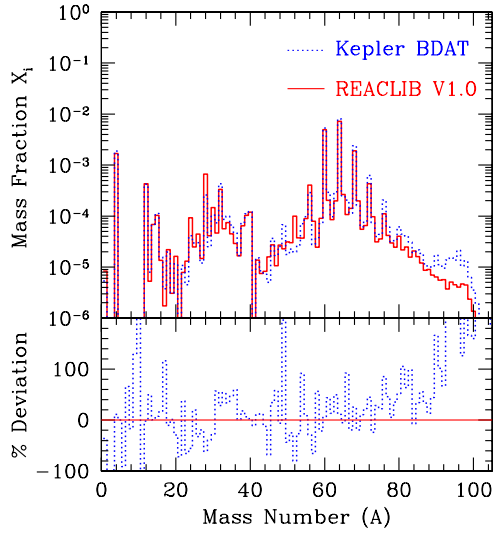

Figure 3. Composition of the burst ashes taken after the last burst, before being further processed by later proximate thermal pulses. The isotopic mass fractions are summed by atomic number for the rate libraries considered and averaged over the hydrogen burning region. The REACLIB V1.0 library is shown in solid lines, while the original KEPLER BDAT library is shown in dotted lines. The deviations in the lower pane are shown relative to the results of the REACLIB V1.0 library.

(A color version of this figure is available in the online journal.)

Overall, the changes in the light curve are not dramatic. As a result, with the currently available updated reaction rates, general conclusions drawn in previous work remain valid. Heger et al. (2007) find overall good agreement between observations of bursts in GS 1826-24 and their model A3. The main deviations are a "shoulder" in the burst rise only seen in the model, and an undershooting of the simulated burst tail compared with observations beyond about 30 s after the burst peak. With the new reaction library we still see the "shoulder" in the rise time. The main significant difference caused by the reaction rate update is a change in the shape of the burst tail about 20–60 s after the burst peak, which likely increases the undershooting compared with observations. While the change is rather small, it might be relevant for attempts to extract the amount of hydrogen burned in the burst from fitting of burst tails.

Another important result of burst calculations is a prediction for the burst ashes setting the composition of the outer crust. This is needed to calculate crustal heating, which has been shown to be quite sensitive to the initial composition set by X-ray bursts (Gupta et al. 2008), and which directly affects observables such as superburst ignition depth and long-term cooling behavior of transients in their off-state (Cumming & Bildsten 2001; Strohmayer & Brown 2002). We calculate an average composition after the last burst integrating over fully burned regions where hydrogen is almost fully consumed (X(H) < 0.01 & X(He) > 0.03). These abundance limits denote the layers in the neutron star surface that have undergone explosive hydrogen burning, but have not been further processed and subsumed into the crust, thus sampling the latest X-ray burst ash composition. A comparison of the composition of the burst ashes predicted with the old and with the new reaction rates is shown in Figure 3. With the new reaction rates significantly less material is processed toward the end of the *rp*-process resulting in significantly reduced abundances beyond $A = 80$. This is largely due to the updated masses in this region, particularly for nuclei relevant for (p, γ) reactions on the waiting point nuclides ^{68}Se, ^{76}Sr, ^{84}Mo, ^{88}Ru, ^{92}Pd, ^{96}Cd, and ^{100}Sn. The proton separation energies for the resulting nuclides in the original Kepler BDAT library are $S_p = -0.0370, -1.2484, -0.4903, -1.0016, -0.8070,$ and -0.4193 MeV, while in the new REACLIB V1.0 library, they are $S_p = -0.6357, -0.0499, -1.2370, -0.7000, -1.2320,$ and -1.3790 MeV, respectively. More importantly, there are significant differences at some specific mass numbers where progenitor reaction rates have changed. With the new reaction rates, ^{28}Si production is significantly increased making it the most abundant isotope with $A < 60$. There is also a new abundance peak at $A = 52$. On the other hand, $A = 24$ production is now reduced.

5. CONCLUSIONS

As part of the REACLIB project we have presented an updated reaction library with new experimental and theoretical proton-, α-, and γ-induced reaction rates for applications in hydrogen and helium burning. The presented REACLIB V1.0 library represents a snapshot of recommended rates in an ongoing process of continuous updates, that is fully tracked and transparently documented. The easy to use Web interface allows users to access the MySQL database to download libraries, perform searches, or compare rates.

As a first application, we also present the first full network, one-dimensional X-ray burst model calculation carried out with a fully documented and publicly available reaction rate set. This calculation can therefore serve as a benchmark to compare different X-ray burst models from different groups as the exact same reaction rate set can be downloaded and used in other calculations. This opens the door for efforts to disentangle nuclear physics uncertainties from uncertainties in numerical treatment and other model features such as implementation of semi-convection.

We demonstrate that despite the significantly updated library there are significant, but not dramatic changes in the calculated prototypical burst X-ray light curves or burst ashes. General

conclusions drawn from previous calculations with the model therefore remain valid. In particular, the "shoulder" in the burst rise, not observed in nature, remains a feature of the model calculations. Significant changes in the light curve do occur at late times, where they tend to increase the discrepancy between model calculations and observations. The fact that the largest change in the light curve occurs in the region where discrepancies with observations have been found before might indicate that this part of the light curve is powered by particularly uncertain nuclear physics. This is not surprising, as at late times the *rp*-process reaction flow involves heavier nuclei further away from stability. This might pose a difficulty for attempts to use the burst tails to determine the amount of hydrogen burned—an important parameter needed to model observed spectra and the Eddington luminosity. Significant changes in the composition of the burst ashes illustrate the need for accurate *rp*-process nuclear physics to reliably estimate the composition of the outer neutron star crust for specific types of bursts.

We would like to emphasize that our study is not a systematic exploration of the sensitivity of burst models to the underlying nuclear physics. Rather, we show results for a burst calculation with updated reaction rates. The changes in the reaction rates discussed here depend on which reaction rate happened to have new experimental or theoretical information and how dramatically this new information impacted the rate. Clearly more work is needed to identify the critical nuclear physics and the impact of nuclear physics uncertainties in X-ray bursts. A first step is the post-processing studies by Parikh et al. (2008) who already use a REACLIB snapshot as one of their reference libraries. Work on a similar study using our full one-dimensional X-ray burst model is underway and is needed to go beyond the post-processing approximation. Such a systematic study will also enable us to identify the specific causes of the burst model changes found in this work. Because of the major computational demands of the burst model calculations, such an analysis is beyond the scope of the present work.

Establishing an updated REACLIB reaction rate library for hydrogen and helium burning is only a first step. Future REACLIB updates will include rates relevant for s- and r-process nucleosynthesis calculations and reaction rate uncertainties. Also, two additional terms in the REACLIB seven-parameter form may be added in order to achieve greater accuracy and precision. Currently one can download libraries in the REACLIB file structure format. As the reaction rate database file structure is different for the Kepler code, we will make available the REACLIB-to-BDAT conversion routines. Also, we have an XML format available, which can be used as a branching point into other formats. Tabular databases can be easily generated once their form is specified. One advantage of analytic forms over tabular forms is their applicability beyond the fitted temperature range, as long as one is careful to adopt "physical" values for parameters. We have here presented fitting rules to ensure such physical behavior. Another advantage applies to reaction rates with low level densities. The transition from direct capture to a low-lying resonance or one resonance to another is not smooth. Interpolating tables present difficulties in accurately reproducing these "kinks" in the reaction rate.

The REACLIB database is meant to serve the community in its nuclear astrophysics needs and to promote data dissemination, evaluation, and the synchronization of nuclear input among the differing astrophysical modelers. Community input is highly desirable.

We thank Sam Austin for helpful discussions and Michael Smith (http://www.nucastrodata.org), Kerstin Sonnabend (CARINA, http://www.ikp.physik.tu-darmstadt.de/carina/), Iris Dillmann (KADoNiS, http://www.kadonis.org), and Boris Pritychenko (NNDC ENDF, http://www.nndc.bnl.gov/astro/) for useful discussions on data availability, evaluation, and dissemination. This work was supported by the U.S. National Science Foundation Grants PHY-01-10253 (NSCL), PHY-02-016783, and PHY-08-22648 (JINA). A.H. was supported in part by US DOE grants DE-FG02-87ER40328 and DE-SC0002300. This work was performed in part under the auspices of the U.S. Department of Energy at Lawrence Livermore National Laboratory under Contract No. DE-AC52-07NA27344. Additional support was granted through the DOE Scientific Discovery through Advanced Computing program (DC-FC02-01ER41176). T.R. and F.K.T were supported by the Swiss NSF grant 200020-122287.

REFERENCES

Aikawa, M., Arnould, M., Goriely, S., Jorissen, A., & Takahashi, K. 2005, A&A, 441, 1195
Allen, B. J., Gibbons, J. H., & Macklin, R. L. 1971, Adv. Nucl. Phys., 4, 205
Angulo, C., et al. 1999, Nucl. Phys. A, 656, 3
Arnould, M., & Goriely, S. 2003, Phys. Rep., 384, 1
Audi, G., Bersillon, O., Blachot, J., & Wapstra, A. H. 2003a, Nucl. Phys. A, 729, 3
Audi, G., Wapstra, A. H., & Thibault, C. 2003b, Nucl. Phys. A, 729, 337
Audouze, J., Truran, J. W., & Zimmerman, B. A. 1973, ApJ, 184, 493
Bao, Z. Y., Beer, H., Käppeler, F., Voss, F., Wisshak, K., & Rauscher, T. 2000, At. Data Nucl. Data Tables, 76, 70
Bao, Z. Y., & Käppeler, F. 1987, At. Data Nucl. Data Tables, 36, 411
Bardayan, D. W., et al. 2000, Phys. Rev. C, 62, 055804
Bardayan, D. W., et al. 2006, Phys. Rev. C, 74, 045804
Bateman, N., et al. 2001, Phys. Rev. C, 63, 035803
Bazin, D., et al. 2008, Phys. Rev. Lett., 101, 252501
Beer, H., Voss, F., & Winters, R. R. 1992, ApJS, 80, 403
Blatt, J. M., & Weisskopf, V. F. 1991, Theoretical Nuclear Physics (New York: Courier Dover Publications)
Block, M., et al. 2008, Nucl. Instrum. Methods Phys. Res. B, 266, 4521
Borrel, V., et al. 1992, Z. Phys., 344, 135
Boyd, R. N. 2008, An Introduction to Nuclear Astrophysics (Chicago, IL: Univ. Chicago Press)
Bradfield-Smith, W., et al. 1999, Phys. Rev. C, 59, 3402
Brown, B. A., Clement, R. R., Schatz, H., Volya, A., & Richter, W. A. 2002, Phys. Rev. C, 65, 045802
Buchmann, L. 1996, ApJ, 468, L127 (erratum 479, L153 [1997])
Buchmann, L. 2008, in Capture Gamma-Ray Spectroscopy and Related Topics, 10th Symposium on Nuclei in the Cosmos, (Trieste: POS), PoS(NICX)009 (http://pos.sissa.it/archive/conferences/053/009/NIC X_009.pdf)
Burbidge, E. M., Burbidge, G. R., Fowler, W. A., & Hoyle, F. 1957, Rev. Mod. Phys., 29, 547
Caggiano, J. A., et al. 2001, Phys. Rev. C, 64, 025802
Cameron, A. G. W. 1957, PASP, 69, 201
Caughlan, G. R., & Fowler, W. A. 1988, At. Data Nucl. Data Tables, 40, 283
Caughlan, G. R., Fowler, W. A., Harris, M. J., & Zimmerman, B. A. 1985, At. Data Nucl. Data Tables, 32, 197
Chae, K. Y., et al. 2009, Phys. Rev. C, 79, 055804
Chafa, A., et al. 2007, Phys. Rev. C, 75, 035810
Chen, A. A., Lewis, R., Swartz, K. B., Visser, D. W., & Parker, P. D. 2001, Phys. Rev. C, 63, 065807
Clark, J. A., et al. 2004, Phys. Rev. Lett., 92, 192501
Clayton, D. D. 1968, Principles of Stellar Evolution and Nucleosynthesis (New York: McGraw-Hill)
Clement, R. R. C., et al. 2004, Phys. Rev. Lett., 92, 172502
Comisel, H., Hategan, C., Graw, G., & Wolter, H. H. 2007, Phys. Rev. C, 75, 045807
Cornelisse, R., et al. 2003, A&A, 405, 1033
Cumming, A., & Bildsten, L. 2001, ApJ, 559, L127
D'Auria, J. M., et al. 2004, Phys. Rev. C, 69, 065803
Davids, B., et al. 2003, Phys. Rev. C, 67, 065808
Descouvemont, P., & Rauscher, T. 2006, Nucl. Phys. A, 777, 137
Diget, C. A., et al. 2009, Phys. Rev. C, 80, 034316

Dillmann, I., Heil, M., Käppeler, F., Plag, R., Rauscher, T., & Thielemann, F.-K. 2006, in AIP Conf. Ser. 819, Capture Gamma-Ray Spectroscopy and Related Topics, ed. A. Woehr & A. Aprahamian (Melville, NY: AIP), 123
Dossat, C., et al. 2007, Nucl. Phys. A, 792, 18
Duflo, J., & Zuker, A. P. 1995, Phys. Rev. C, 52, 23
Dufour, M., & Descouvemont, P. 2004, Nucl. Phys. A, 730, 316
Elomaa, V.-V., et al. 2009, Phys. Rev. Lett., 102, 252501
Evans, W. D., Belian, R. D., & Conner, J. P. 1976, ApJ, 207, L91
Fisker, J. L., Barnard, V., Görres, J., Langanke, K., Martínez-Pinedo, G., & Wiescher, M. C. 2001, At. Data Nucl. Data Tables, 79, 241
Fisker, J. L., Schatz, H., & Thielemann, F.-K. 2008, ApJS, 174, 261
Fisker, J. L., Tan, W., Görres, J., Wiescher, M., & Cooper, R. L. 2007, ApJ, 665, 637
Forstner, O., Herndl, H., Oberhummer, H., Schatz, H., & Brown, B. A. 2001, Phys. Rev. C, 64, 045801
Fowler, W. A., Caughlan, G. R., & Zimmerman, B. A. 1967, ARA&A, 5, 525
Fowler, W. A., Caughlan, G. R., & Zimmerman, B. A. 1975, ARA&A, 13, 69
Fox, C., Iliadis, C., Champagne, A. E., Fitzgerald, R. P., Longland, R., Newton, J., Pollanen, J., & Runkle, R. 2005, Phys. Rev. C, 71, 055801
Freer, M., et al. 2009, Phys. Rev. C, 80, 041303
Fröhlich, C., Martínez-Pinedo, G., Liebendörfer, M., Thielemann, F.-K., Bravo, E., Hix, W. R., Langanke, K., & Zinner, N. T. 2006, Phys. Rev. Lett., 96, 142502
Fuller, G. M., Fowler, W. A., & Newman, M. J. 1980, ApJS, 42, 447
Fuller, G. M., Fowler, W. A., & Newman, M. J. 1982a, ApJ, 252, 715
Fuller, G. M., Fowler, W. A., & Newman, M. J. 1982b, ApJS, 48, 279
Fuller, G. M., Fowler, W. A., & Newman, M. J. 1985, ApJ, 293, 1
Fynbo, H. O. U., et al. 2005, Nature, 433, 136
Gomi, T., et al. 2005, Nucl. Phys. A, 758, 761
Goriely, S. 1998, Phys. Lett. B, 436, 10
Görres, J., Arlandini, C., Giesen, U., Heil, M., Käppeler, F., Leiste, H., Stech, E., & Wiescher, M. 2000, Phys. Rev. C, 62, 055801
Görres, J., Wiescher, M., & Thielemann, F.-K. 1995, Phys. Rev. C, 51, 392
Grindlay, J. E. 1976, Comments Astrophys., 6, 165
Guo, B., Li, Z. H., Bai, X. X., Liu, W. P., Shu, N. C., & Chen, Y. S. 2006, Phys. Rev. C, 73, 048801
Gupta, S. S., Kawano, T., & Möller, P. 2008, Phys. Rev. Lett., 101, 231101
Hahn, K. I., et al. 1996, Phys. Rev. C, 54, 1999
Hale, S. E., Champagne, A. E., Iliadis, C., Hansper, V. Y., Powell, D. C., & Blackmon, J. C. 2004, Phys. Rev. C, 70, 045802
Hansen, C. J., & van Horn, H. M. 1975, ApJ, 195, 735
Harris, M. J., Fowler, W. A., Caughlan, G. R., & Zimmerman, B. A. 1983, ARA&A, 21, 165
Hauser, W., & Feshbach, H. 1952, Phys. Rev., 87, 366
Heger, A., Cumming, A., Galloway, D. K., & Woosley, S. E. 2007, ApJ, 671, L141
Hencheck, M., et al. 1994, Phys. Rev. C, 50, 2219
Herndl, H., & Brown, B. A. 1997, Nucl. Phys. A, 627, 35
Herndl, H., Görres, J., Wiescher, M., Brown, B. A., & van Wormer, L. 1995, Phys. Rev. C, 52, 1078
Hoffman, J. A., Cominsky, L., & Lewin, W. H. G. 1980, ApJ, 240, L27
Holmes, J. A., Woosley, S. E., Fowler, W. A., & Zimmerman, B. A. 1976, At. Data Nucl. Data Tables, 18, 305
Howard, W. M., Arnett, W. D., & Clayton, D. D. 1971, ApJ, 165, 495
Iliadis, C. 2007, Nuclear Physics of Stars (New York: Wiley-VCH)
Iliadis, C., D'Auria, J. M., Starrfield, S., Thompson, W. J., & Wiescher, M. 2001, ApJS, 134, 151
Imbriani, G., et al. 2005, Eur. Phys. J. A, 25, 455
Janas, Z., et al. 1999, Phys. Rev. Lett., 82, 295
Jänecke, J., & Masson, P. J. 1988, At. Data Nucl. Data Tables, 39, 265
Jenkins, D. G., et al. 2004, Phys. Rev. Lett., 92, 031101
Jenkins, D. G., et al. 2006, Phys. Rev. C, 73, 065802
Joss, P. C. 1977, Nature, 270, 310
Kellerbauer, A., et al. 2007, Phys. Rev. C, 76, 045504
Kiss, G. G., Rauscher, T., Gyürky, G., Simon, A., Fülöp, Z., & Somorjai, E. 2008, Phys. Rev. Lett., 101, 191101
Kunz, R., Fey, M., Jaeger, M., Mayer, A., Hammer, J. W., Staudt, G., Harissopulos, S., & Paradellis, T. 2002, ApJ, 567, 643
Kunz, R., Jaeger, M., Mayer, A., Hammer, J. W., Staudt, G., Harissopulos, S., & Paradellis, T. 2001, Phys. Rev. Lett., 86, 3244
Kuulkers, E., Homan, J., van der Klis, M., Lewin, W. H. G., & Méndez, M. 2002, A&A, 382, 947
Lewitowicz, M., et al. 1995, Nucl. Phys. A, 588, c197
Li, Z. H., et al. 2006, Phys. Rev. C, 74, 035801
Liddick, S. N., et al. 2006, Phys. Rev. Lett., 97, 082501
LUNA Collaboration, et al. 2006, Nucl. Phys. A, 779, 297
Ma, Z., et al. 2007, Phys. Rev. C, 76, 015803
Mao, Z. Q., Fortune, H. T., & Lacaze, A. G. 1995, Phys. Rev. Lett., 74, 3760
Marta, M., et al. 2008, Phys. Rev. C, 78, 022802
Martın, A., et al. 2007, Eur. Phys. J. A, 34, 341
Mazzocchi, C., et al. 2007, Phys. Rev. Lett., 98, 212501
Moazen, B. H., et al. 2007, Phys. Rev. C, 75, 065801
Mocelj, D., Rauscher, T., Martínez-Pinedo, G., Langanke, K., Pacearescu, L., Faessler, A., Thielemann, F.-K., & Alhassid, Y. 2007, Phys. Rev. C, 75, 045805
Mohr, P. 2007, Eur. Phys. J. A, 31, 23
Möller, P., Nix, J. R., & Kratz, K.-L. 1997, At. Data Nucl. Data Tables, 66, 131
Möller, P., Nix, J. R., Myers, W. D., & Swiatecki, W. J. 1995, At. Data Nucl. Data Tables, 59, 185
Möller, P., Pfeiffer, B., & Kratz, K.-L. 2003, Phys. Rev. C, 67, 055802
Pagel, B. E. J. 1997, Nucleosynthesis and Chemical Evolution of Galaxies (Cambridge: Cambridge Univ. Press)
Parikh, A., José, J., Moreno, F., & Iliadis, C. 2008, New Astron. Rev., 52, 409
Parpottas, Y., Grimes, S. M., Al-Quraishi, S., Brune, C. R., Massey, T. N., Oldendick, J. E., Salas, A., & Wheeler, R. T. 2004, Phys. Rev. C, 70, 065805
Parpottas, Y., Grimes, S. M., Al-Quraishi, S., Brune, C. R., Massey, T. N., Oldendick, J. E., Salas, A., & Wheeler, R. T. 2006, Phys. Rev. C, 73, 049907
Pruet, J., & Fuller, G. M. 2003, ApJS, 149, 189
Pruet, J., Hoffman, R. D., Woosley, S. E., Janka, H.-T., & Buras, R. 2006, ApJ, 644, 1028
Rauscher, T. 2008a, Online code NON-SMOKER$^{\rm WEB}$,version 5.0w and higher, http://nucastro.org/websmoker.html
Rauscher, T. 2008b, Phys. Rev. C, 78, 032801
Rauscher, T. 2008c, J. Phys. G, 35, 014026
Rauscher, T., Kiss, G. G., Gy, G., Simon, A., Fülöp, Z., & Somorjai, E. 2009, Phys. Rev. C, 80, 035801
Rauscher, T., & Thielemann, F.-K. 1998, in Stellar Evolution, Stellar Explosions and Galactic Chemical Evolution, ed. A. Mezzacappa (Bristol: IOP), 519
Rauscher, T., & Thielemann, F.-K. 2000, At. Data Nucl. Data Tables, 75, 1
Rauscher, T., Thielemann, F.-K., & Kratz, K.-L. 1997, Phys. Rev. C, 56, 1613
Rehm, K. E., et al. 1998, Phys. Rev. Lett., 80, 676
Ringle, R., et al. 2007, Phys. Rev. C, 75, 055503
Rodríguez, D., et al. 2004, Phys. Rev. Lett., 93, 161104
Rolfs, C. E., & Rodney, W. S. 1988, Cauldrons in the Cosmos: Nuclear Astrophysics (Chicago, IL: Univ. Chicago Press)
Runkle, R. C., Champagne, A. E., Angulo, C., Fox, C., Iliadis, C., Longland, R., & Pollanen, J. 2005, Phys. Rev. Lett., 94, 082503
Rykaczewski, K., et al. 1995, Phys. Rev. C, 52, 2310
Schatz, H. 2006, Int. J. Mass Spectrom., 251, 293
Schatz, H., Bertulani, C. A., Brown, B. A., Clement, R. R., Sakharuk, A. A., & Sherrill, B. M. 2005, Phys. Rev. C, 72, 065804
Schatz, H., & Rehm, K. E. 2006, Nucl. Phys. A, 777, 601
Schatz, H., et al. 1998, Phys. Rep., 294, 167
Schatz, H., et al. 2001, Phys. Rev. Lett., 86, 3471
Schürmann, D., et al. 2005a, Eur. Phys. J. A, 26, 301
Schürmann, D., et al. 2005b, Nucl. Phys. A, 758, 367
Schury, P., et al. 2007, Phys. Rev. C, 75, 055801
Sikler, G., et al. 2005, Nucl. Phys. A, 763, 45
Smith, E., et al. 2006, in International Symp. on Nuclear Astrophysics, Nuclei in the Cosmos IX, ed. J. Cederkall (Geneva: CERN), 179
Smith, M. S., et al. 2008, in AIP Conf. Ser. 1016, Origin of Matter and Evolution of Galaxies, ed. T. Suda, T. Nozawa, A. Ohnishi, K. Kato, M. Y. Fujimoto, T. Kajino, & S. Kubono (Melville, NY: AIP), 466
Stadlmann, J., et al. 2004, Phys. Lett. B, 586, 27
Strohmayer, T., & Bildsten, L. 2006, in Compact Stellar X-ray Sources, ed. W. H. G. Lewin & M. van der Klis (Cambridge Astrophys. Ser. 39, Cambridge: Cambridge Univ. Press), 113
Strohmayer, T. E., & Brown, E. F. 2002, ApJ, 566, 1045
Sztajno, M., van Paradijs, J., Lewin, W. H. G., Trumper, J., Stollman, G., Pietsch, W., & van der Klis, M. 1985, ApJ, 299, 487
Takahashi, K., & Yokoi, K. 1987, At. Data Nucl. Data Tables, 36, 375
Tan, W. P., Fisker, J. L., Görres, J., Couder, M., & Wiescher, M. 2007, Phys. Rev. Lett., 98, 242503
Tang, X., et al. 2004, Phys. Rev. C, 69, 055807
Tang, X., et al. 2008, in AIP Conf. Ser. 972, Exotic Nuclei and Nuclear/Particle Astrophysics (II), ed. L. Trache & S. Stoica (Melville, NY: AIP), 261
Tang, X. D., et al. 2007, Phys. Rev. Lett., 99, 052502
Thielemann, F.-K., Arnould, M., & Truran, J. 1987, in Advances in Nuclear Astrophysics, ed. A. Vangioni-Flam (Gif-sur-Yvette: Editions Frontiére), 525
Tuli, J. K., & National Nuclear Data Center, 2007, Nuclear Wallet Cards (Uptan, NY: NNDC), http://www.nndc.bnl.gov/wallet

van Paradijs, J., Sztajno, M., Lewin, W. H. G., Trumper, J., Vacca, W. D., & van der Klis, M. 1986, MNRAS, 221, 617
van Wormer, L., Goerres, J., Iliadis, C., Wiescher, M., & Thielemann, F.-K. 1994, ApJ, 432, 326
Wagoner, R. V. 1969, ApJS, 18, 247
Wallace, R. K., & Woosley, S. E. 1981, ApJS, 45, 389
Wallerstein, G., et al. 1997, Rev. Mod. Phys., 69, 995
Wapstra, A. H., Audi, G., & Thibault, C. 2003, Nucl. Phys. A, 729, 129
Watts, A. L., & Maurer, I. 2007, A&A, 467, L33
Weinberg, N. N., Bildsten, L., & Schatz, H. 2006, ApJ, 639, 1018
Wiescher, M., Gorres, J., Thielemann, F.-K., & Ritter, H. 1986, A&A, 160, 56
Wilmes, S., Wilmes, V., Staudt, G., Mohr, P., & Hammer, J. W. 2002, Phys. Rev. C, 66, 065802
Woosley, S. E., Fowler, W. A., Holmes, J. A., & Zimmerman, B. A. 1978, At. Data Nucl. Data Tables, 22, 371
Woosley, S. E., Hartmann, D. H., Hoffman, R. D., & Haxton, W. C. 1990, ApJ, 356, 272
Woosley, S. E., & Hoffman, R. D. 1992, ApJ, 395, 202
Woosley, S. E., & Taam, R. E. 1976, Nature, 263, 101
Woosley, S. E., et al. 2004, ApJS, 151, 75
Zhou, X. G., Dejbakhsh, H., Gagliardi, C. A., Jiang, J., Trache, L., & Tribble, R. E. 1996, Phys. Rev. C, 53, 982